Electronic Supplementary Material (ESI) for Nanoscale Advances.

Supplementary information

Tuning morphology, stability and optical properties of $CsSnBr_3$ nanocrystals through bismuth doping for visible-light-driven applications

Md. Asif Adib, Fahmida Sharmin, and M. A. Basith*

Nanotechnology Research Laboratory, Department of Physics, Bangladesh University of Engineering and Technology, Dhaka 1000, Bangladesh

S1 Photocatalytic dye degradation experiment

Initially, 1.2 mg of RhB was dissolved in 100 ml of distilled water. The concentration of RhB in the solution was then determined by measuring its absorbance spectrum using a UV-vis spectrophotometer Thereafter, 40 mg photocatalyst was added into 50 ml of RhB solution followed by stirring of the solution in dark condition for 1 h to achieve an adsorption-desorption equilibrium between the photocatalyst and RhB. After that, the photocatalytic process was initiated by irradiating the solution using a 500 W Hg-Xn (Hamamatsu L8288) lamp as a solar simulator with an irradiance value of 100 $mWcm^{-2}$ in the visible spectrum. After 30 minutes of illumination, 4 ml of suspension was extracted and centrifuged at 6500 rpm for 2 min. The absorbance spectrum of the mixture was then measured to determine the concentration of the remaining RhB. This same process was carried out for 4 h at 30-minute intervals.

S2 Photocatalytic degradation experiment of Ciprofloxacin

In this case, 1 mg of CIP was dissolved in 100 ml of distilled water to create a CIP solution, and 15 mg of photocatalyst was added into 50 ml of CIP solution. All the other procedures were the same as described in S1.

S3 Active species trapping experiment

Active species trapping experiments were carried out under solar illumination in the presence of four different scavengers: hydroxyl (•OH), superoxide radical ($•O_2^-$), electrons (e^-), and holes (h^+). The change in degradation efficiency was investigated by adding 1.0 mM of IPA (a quencher of •OH), Acrylamide (a quencher of $•O_2^-$), $K_2Cr_2O_7$ (a quencher of e^-), and EDTA – 2Na (a quencher of h^+), respectively.

S4 Electrochemical measurements

The electrochemical impedance spectroscopy and Mott-Schottky measurements of the CSB and CSB′B were conducted in a standard three-electrode system where a sample-coated graphite rod, a platinum wire, and Ag/AgCl were used as the working electrode, the counter electrode and the reference electrode, respectively. For preparing the working electrode, at first a homogenous slurry was made containing 4 mg of prepared sample (80% w/w), 1 mg of ployvinaylidene fluoride (PVDF; 20% w/w) as the binder, and 40 µL of 1-Methyl-2-pyrrolidone (NMP) solution. Then the 5 µL of the slurry was uniformly cast on a graphite rod with an exposed area of ~0.28 cm^{-2} and finally dried at 60 ℃ in an oven.

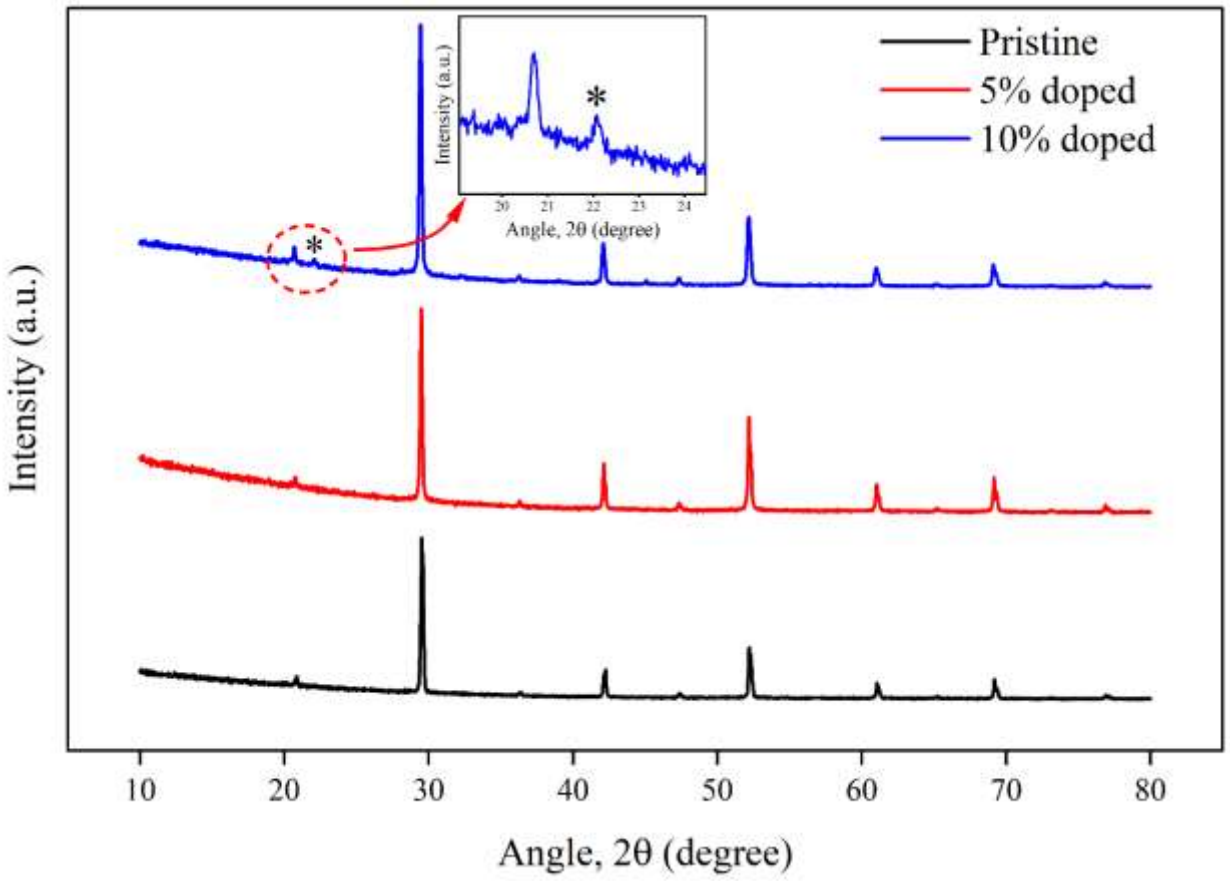

Fig. S1: XRD patterns of the pristine, 5%, and 10% Bi doped nanocrystals. The magnified view of the impurity peak is marked with an asterisk and shown in the inset.

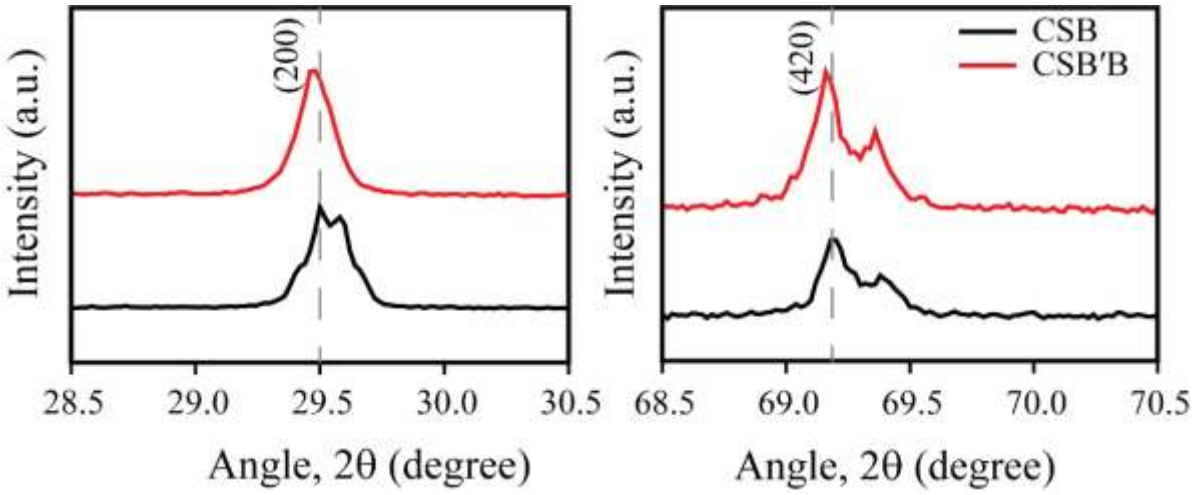

Fig. S2: Magnified view of the XRD patterns of CSB and CSB′B.

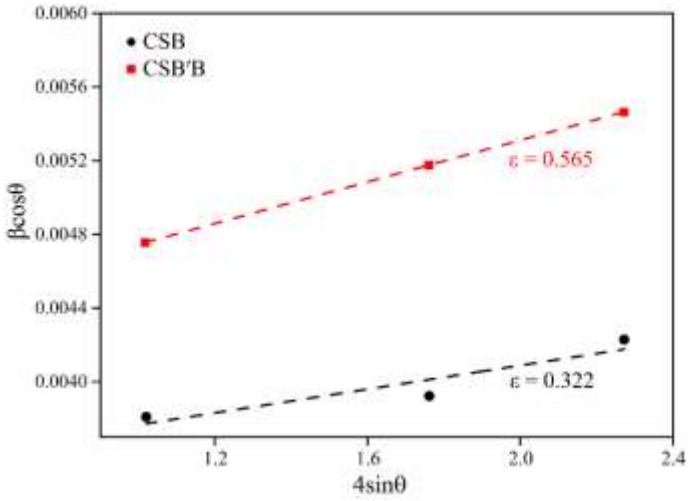

Fig. S3: Williamson-Hall plot for microstrain calculation.

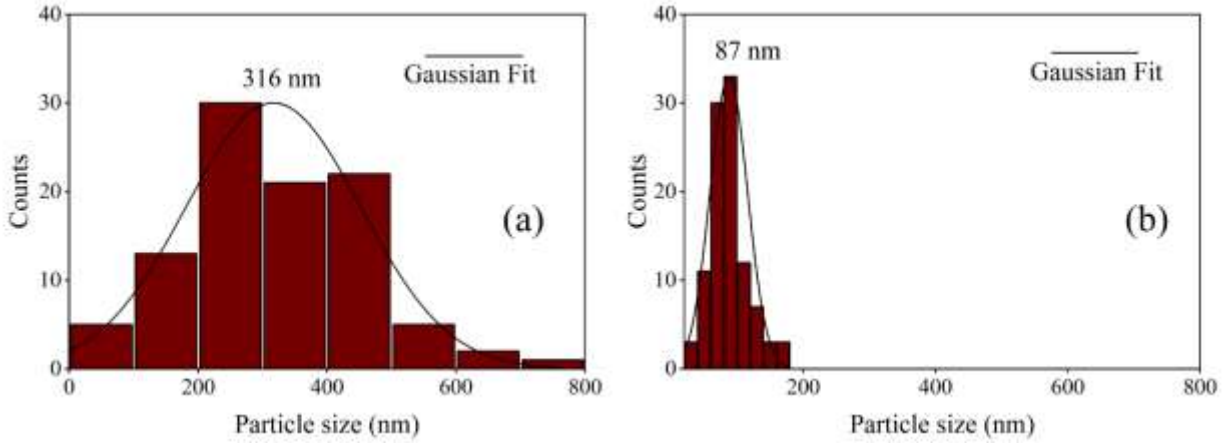

Fig. S4: Particle size distribution of (a) CSB and (b) CSB′B.

Table S1: Mass and atomic percentages of CSB nanocrystals as obtained from EDX analysis.

Element	Mass (%) Theoretical	Mass (%) Experimental	Atom (%) Theoretical	Atom (%) Experimental
Cs	27.05	35.49	20	28.65
Sn	24.16	22.45	20	16.83
Br	48.79	42.06	60	54.51
Total	100	100	100	100

Table S2: Mass and atomic percentages of CSB′B nanocrystals as obtained from EDX analysis.

Element	Mass (%) Theoretical	Mass (%) Experimental	Atom (%) Theoretical	Atom (%) Experimental
Cs	26.9	27.49	20	23.51
Sn	22.74	19.9	19	17.08
Bi	2.02	2.35	1	0.71
Br	48.34	50.26	60	58.7
Total	100	100	100	100

Table S3: Comparison of the interplanar spacing obtained from XRD and SAED pattern.

Crystal Plane	Interplanar spacing (Å)		
	From XRD pattern of CSB	From SAED pattern	
		CSB	CSB′B
(200)	3.03	3.03	3.04
(211)	2.46	2.46	2.46
(420)	1.35	1.35	1.36

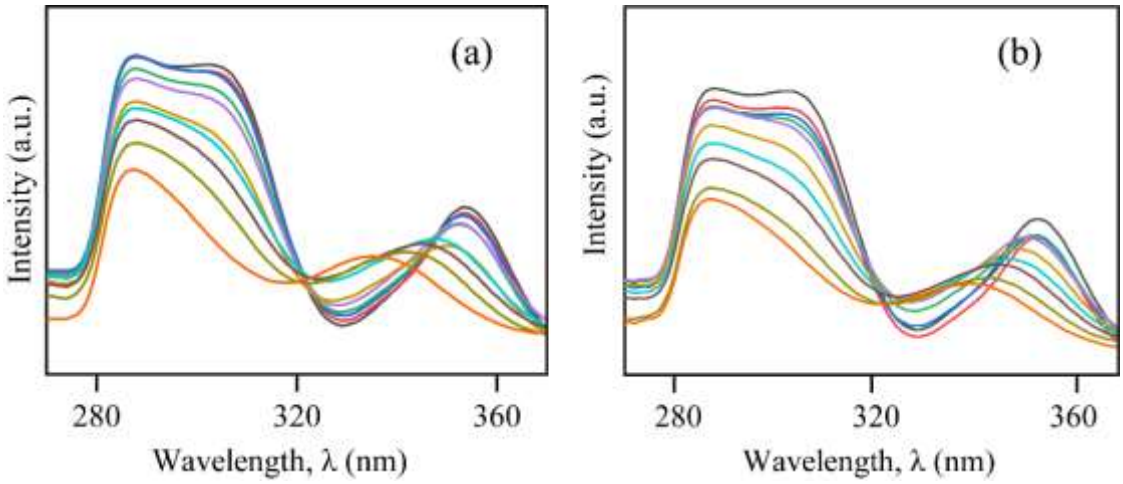

Fig. S5: Spectral changes in the RhB solution containing (a) CSB, and (b) CSB′B under UV-vis irradiation.

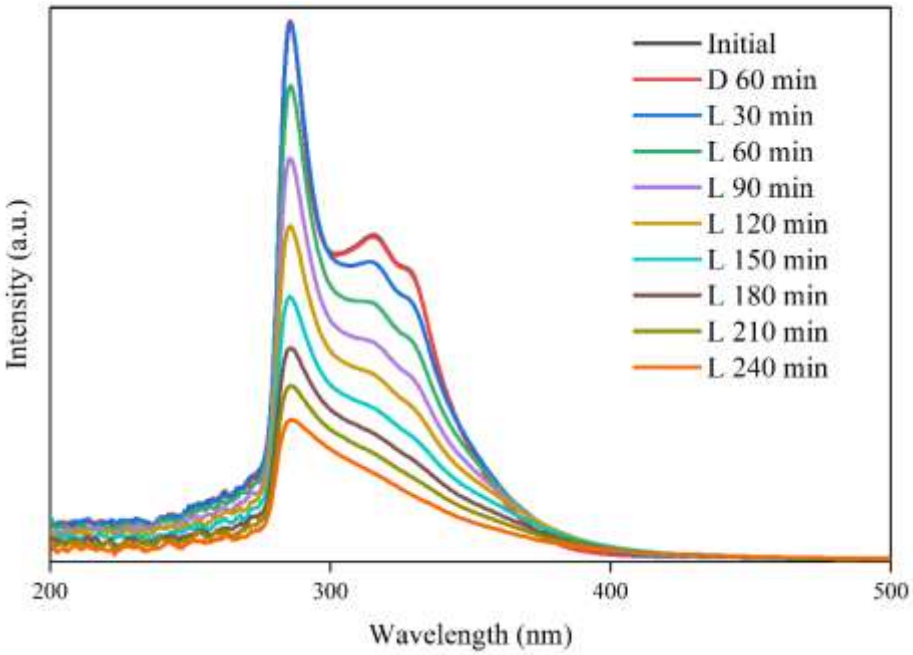

Fig. S6: Spectral change in the Ciprofloxacin solution in the presence of CSB′B under UV-vis irradiation.

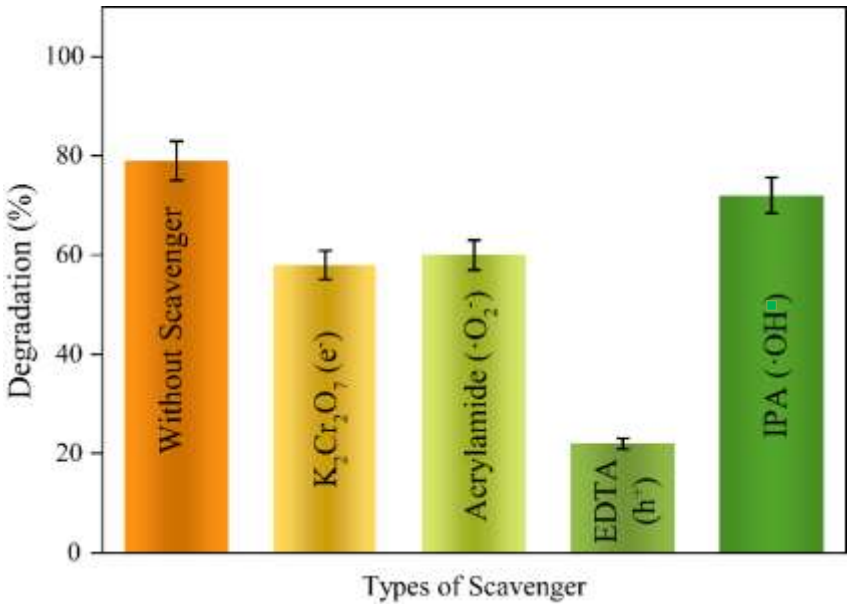

Fig. S7: Change in RhB degradation percentage due to the absence or presence of different scavengers.

Table S4: Pseudo first-order rate constant per minute of CSB, CSB′B, and P25 under UV-vis and visible irradiation.

Sample	Under UV-visible spectrum		Under visible spectrum	
	Efficiency	Rate constant (min^{-1}) (10^{-3})	Efficiency	Rate constant (min^{-1}) (10^{-3})
P25 Titania	93%	11.06	8%	0.35
CSB	68%	5.97	25%	0.89
CSB′B	79%	6.58	42%	1.64

Table S5: Comparison between the experimentally and theoretically obtained structural parameters, optical and electronic band gap values of CSB and CSB′B.

Sample		Structural parameters		Optical Band gap (eV)	Electronic Band gap (eV)
		Lattice parameters (Å)	Volume ($Å^3$)		
CSB	Experimental	6.05	221.66	1.89	--
	Theoretical	5.89	204.44	0.89	0.643
CSB′B	Experimental	6.07	223.23	1.73	--
	Theoretical	5.91	206.43	0.87	0.469

S5 Electron charge density

To investigate the chemical bond nature between the constituent atoms, we have further calculated the Mulliken effective charge calculation. For the CSB sample, the Mulliken effective charge of the constituent atoms Cs, Sn, and Br was found to be 0.45, 0.52, -0.32, and for the CSB′B sample the effective charge of these atoms was found to be 0.47, 0.51, -0.33. Additionally for Bi, the charge was found as 0.45. These values are significantly lower than their formal charge of +1 for Cs, +2 for Sn, -1 for Br, and +3 for Bi. This large discrepancy indicates the presence of mixed ionic and covalent bonding with covalent dominance in the samples [1,2]. From the electron density mapping, as shown in Fig. S8, it can be observed that the electrons of Bi^{3+} overlap with the surrounding Br^- at a greater degree compared to the nearby Sn^{2+}, which indicates the formation of stronger sigma-type Bi-Br covalent bond in the CSB′B perovskite [3-4].

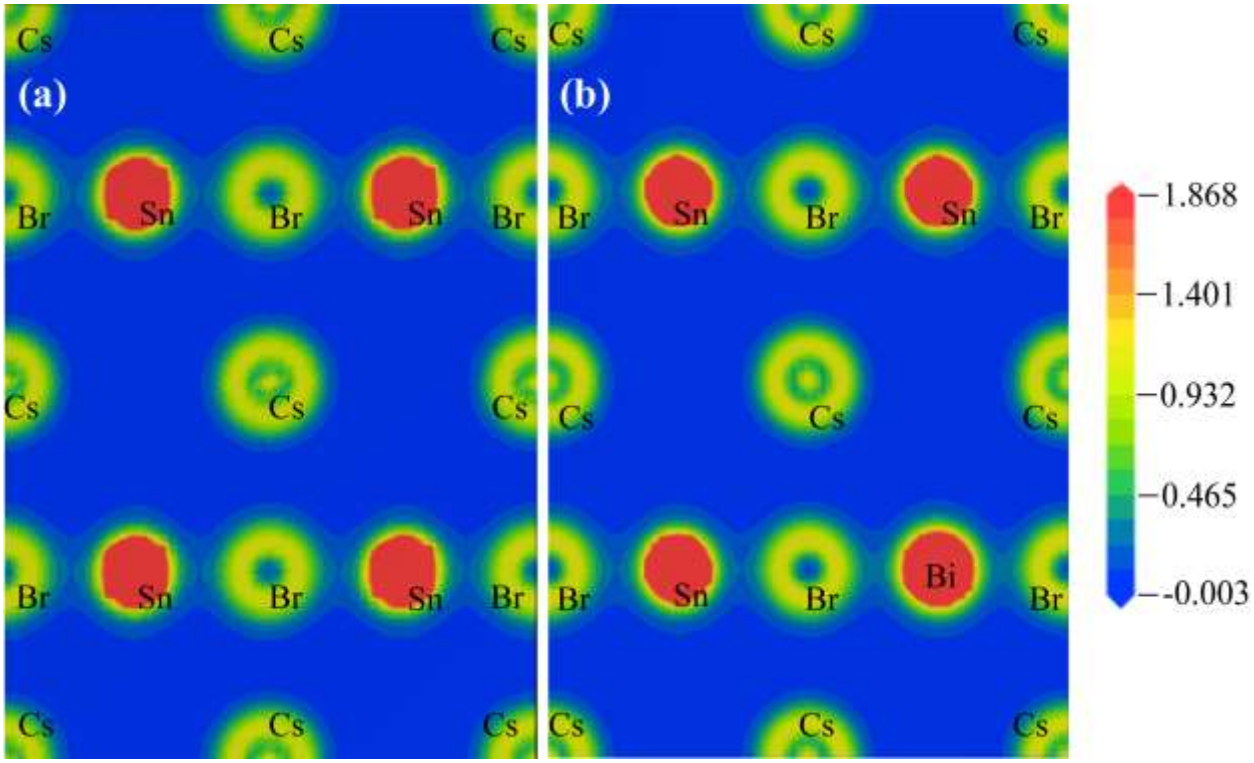

Fig. S8: Electron density mapping along (110) plane of (a) CSB, and (b) CSB′B

Table S6: Variation of analytical parameters with increasing U_{eff}.

Parameters	Experimental value	U_{eff} = 0 eV	U_{eff} = 4 eV	U_{eff} = 5 eV
Lattice parameters (Å)	6.05	5.89	6.06	6.65
Optical band gap (eV)	1.89	0.89	1.83	2.96
Electronic band gap (eV)	--	0.64	1.88	3.49

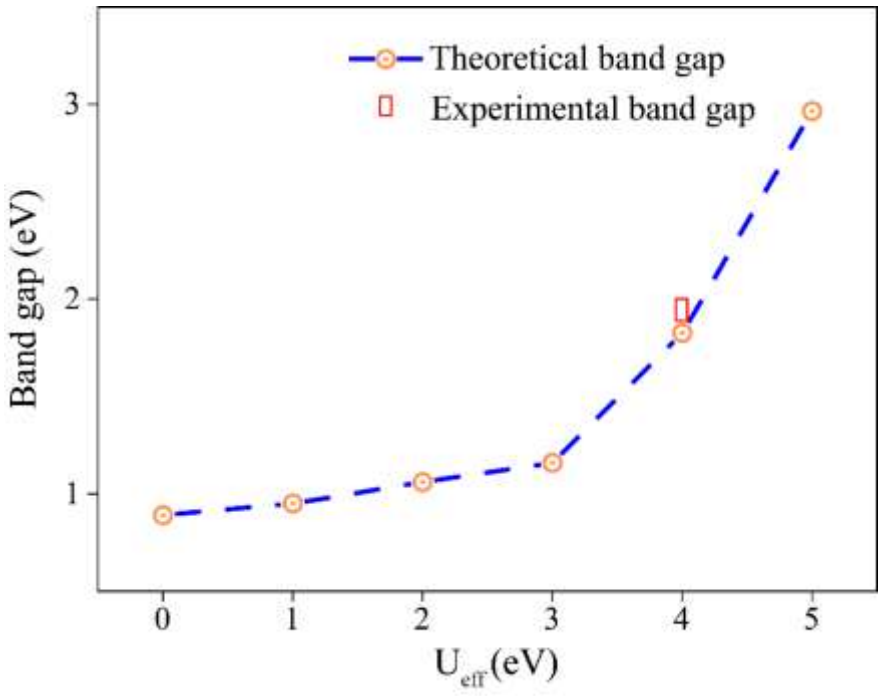

Fig. S9: Optical band gap variation of CSB with U_{eff} = 0 – 5 eV.

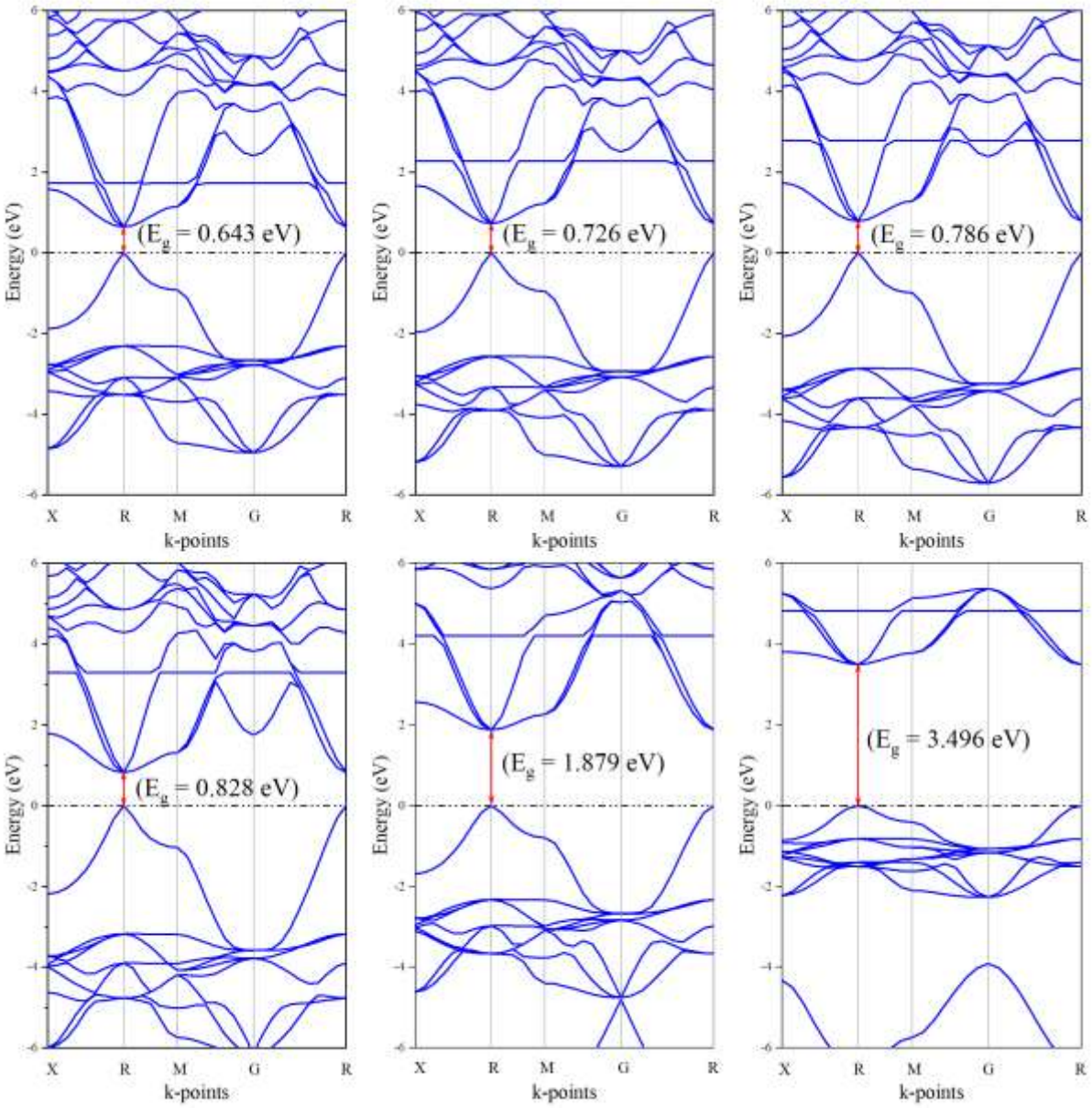

Fig. S10: Variation of the electronic band structure of CSB for U_{eff} = 0 – 5 eV.

References

[1] M. Segall, R. Shah, C. J. Pickard and M. Payne, Population analysis of plane-wave electronic structure calculations of bulk materials, *Phys. Rev. B*, 1996, **54**, 16317.

[2] R. S. Mulliken, Electronic population analysis on LCAO–MO molecular wave functions. I, *J. Chem. Phys.*, 1955, **23**, 1833–1840.

[3] G. M. Dalpian, Q. Liu, C. C. Stoumpos, A. P. Douvalis, M. Balasubramanian, M. G. Kanatzidis and A. Zunger, Changes in charge density vs changes in formal oxidation states: The case of Sn halide perovskites and their ordered vacancy analogues, *Phys. Rev. Materials*, 2017, **1**, 025401.

[4] M. S. Ali, S. Das, Y. F. Abed and M. A. Basith, Lead-free CsSnCl3 perovskite nanocrystals: rapid synthesis, experimental characterization and DFT simulations, *Phys. Chem. Chem. Phys.*, 2021, **23**, 22184–22198.